The Journal of Foot & Ankle Surgery

ORIGINAL ARTICLES

Biomechanics of the First Ray Part V: The Effect of Equinus Deformity

A 3-Dimensional Kinematic Study on a Cadaver Model

Cherie H. Johnson, DPM, FACFAS,[1] and Jeffrey C. Christensen, DPM, FACFAS[2]

The positional change of the medial column of the foot in closed kinetic chain with variable Achilles tendon tension was investigated in seven fresh frozen cadaver specimens using a 3-dimensional radio wave tracking system. The distal tibia and fibula and the intact ankle and foot and were mounted on a non-metallic loading frame. The frame allowed positioning of the foot to simulate midstance phase of gait while the tibia and fibula were axially loaded to 400 N. To record osseous motion, receiving transducers were attached to the first metatarsal, medial cuneiform, navicular, and talus. Movements of these bones in 3-dimensional space were measured as specimens were axially loaded and midstance motor function was simulated using pneumatic actuators. To simulate a progressive equinus influence, force was applied to the Achilles tendon at tensile loads of 0%, 30%, and 60% of predicted maximum strength during each test trial. Osseous positions and orientations were collected and analyzed in all three cardinal planes utilizing data recorded. As Achilles load increased, the position of the first metatarsal became significantly more inverted ($P < .05$*). Although not statistically significant, remarkable trends of arch flattening motion were detected in the distal segments of the medial column with varied Achilles load. Increased Achilles load reduced the influence of peroneus longus on the medial column.* (The Journal of Foot & Ankle Surgery 44(1):114-120, 2005)

Key words: first ray hypermobility, foot biomechanics, equinus, peroneus longus, tarsal movements

Equinus deformity is the most profound causal agent in foot pathomechanics and is frequently linked to common foot pathology (1–3). With the Achilles tethering ankle joint dorsiflexion, pathologic forces of equinus are transmitted through the foot. Intuitively, as a result of structural variability of the arch, it is felt that an identical destructive influence can induce a variety of pathological compensations. These include Achilles tendinopathy (4), posterior tibial tendonitis (4), flatfoot conditions (1, 5, 6), plantar fasciitis (4), Lisfranc arthrosis (5), Charcot arthropathy (7–9), hallux valgus (10), hallux limitus (11), plantar ulcerations (9, 12–14), forefoot calluses (4, 11), metatarsalgia (4, 6), and hammertoe contractures (15). Although equinus is blamed for the genesis of various foot deformities, cause-and-effect relationships have not been thoroughly investigated.

From Northwest Surgical Biomechanics Research Laboratory, Swedish Medical Center, Seattle, WA. Address correspondence to: Jeffrey C. Christensen, DPM, FACFAS, Northwest Surgical Biomechanics Laboratory, Swedish Medical Center, Providence Campus, Graduate Medical Education, 500–17th Ave, Seattle, WA 98122. E-mail: jccdpm@yahoo.com

[1]Director of Podiatric Medical Education; Attending Surgeon, Division of Podiatry, Department of Orthopedics, Swedish Medical Center, Seattle, WA.

[2]Director, Northwest Surgical Biomechanics Laboratory; Attending Surgeon, Division of Podiatry, Department of Orthopedics, Swedish Medical Center, Seattle, WA.

1067-2516/05/4401-0003$30.00/0

doi:10.1053/j.jfas.2005.01.003

Biomechanical Influence of Triceps Surae

The triceps surae functions across the ankle and subtalar joints with the gastrocnemius component affecting the knee as well (8). The gastrocnemius muscle is the most consistently active muscle during static stance due to the center of gravity projecting anterior to the ankle (16, 17). The maximum forces attained by the gastrosoleal complex are: medial head of gastrocnemius 500 N, lateral head of gastrocnemius 700 N, and soleus 900 N.

Approximately 450 N of tension is created by the Achilles tendon during midstance (18).

Equinus

Equinus deformity is defined as the inability to dorsiflex the ankle sufficiently enough to allow the heel to contact the supporting surface without subtalar or midtarsal joint pronation (19). Controversy exists regarding the magnitude of equinus that is clinically important. Nonetheless, there is a strong consensus that the ankle must dorsiflex past perpendicular for smooth ambulation. Schuster described the amount of ankle motion needed in walking as the "walking angle"(20). Because values for normal vary in the literature, the normal amount of ankle motion is best described as a range of values between 3 to 15 degrees of dorsiflexion past perpendicular (19, 21–33). Hansen theorized a tight Achilles tendon as an atavistic trait similar to how Lapidus attributed first ray malalignment to atavism (10, 34–36).

The effects of treating equinus were studied by Sgarlato, who found that tendo Achilles lengthening (TAL) relieved calf and arch pain, leg fatigue, plantar keratomas, symptoms from hallux valgus deformity and tarsal coalition. This is one of the few studies that has attempted to evaluate the cause and effect relationship of equinus and foot pathology. Unfortunately, the TAL was done in conjunction with other procedures that contribute many variables (11).

Compensation for Equinus

The subtle pathomechanics of a shortened gastrocnemius aponeurosis has been known for over 100 years (37). Since these early descriptions, the various types of equinus compensations have become more clearly understood. Common modes of compensation for lack of ankle dorsiflexion include triplanar rearfoot motion (pronation), hypermobile flatfoot, an early heel-off (bouncy gait), and an abducted gait pattern (1, 19, 38). Proximal compensatory mechanisms for equinus have also been described, including lumbar lordosis, hip flexion, and genu recurvatum (9). If only partially compensated, an equinus deformity will result in increased forefoot load causing calluses, metatarsalgia, and forefoot ulcerations (6, 13, 19, 38–40).

Opposing Forces

An antagonistic relationship exists between the triceps surae and the structures of arch retention. These structures include tibialis posterior, peroneus longus, plantar fascia, and the plantar ligaments. In open kinetic chain, Duchenne described Achilles and peroneus longus as having opposing roles (24). While in closed kinetic chain, investigators have observed the triceps as having an arch-flattening effect (26, 41). Thus, the analogy of a "tug-o-war" can be used to describe the triceps surae along with weight bearing load vs. their antagonists and other structures of arch retention.

As determined by dynamic electromyography, the tibialis posterior fires at approximately 10% of the gait cycle, while the gastrosoleus contracts later (42). Thus, a foot with an equinus influence will generate premature passive loading of the Achilles applied to the arch from foot flat to heel lift in addition to the normal dynamic loads. This passive influence can oppose the active function of the tibialis posterior and lead to arch insufficiency (43, 44).

First Ray Hypermobility

Although Duchenne described first ray mobility in the 1800s by stating, "The joints of the medial border of the forefoot have a certain amount of vertical motion," (24) Morton advanced the concept of first ray hypermobility. Morton's criteria for hypermobility of the first ray included clinically demonstrable "hyperextension" (dorsiflexion of the first ray), widening of the space between the first and second cuneiforms, and a thickened second metatarsal shaft (28, 45–47).

First ray motion has been studied by numerous investigators (19, 48–53). Klaue et al suggested a direct relationship between painful hallux valgus deformity and hypermobility of the first metatarsocuneiform joint (52). Thordarson et al, through the use of a 3-dimensional tracking system, found that the unopposed pull of peroneus longus consistently abducted the forefoot in the transverse plane (41).

In Part I in this series of investigations on biomechanics of the first ray, the authors found peroneus longus to evert the medial column creating a locking effect of the first ray (54). In Part II, the intermetatarsal angle was demonstrated to have an influence on mobility of the first ray (55). Part III demonstrated that arthrodesis of the first metatarasocuneiform joint increases the efficiency of peroneus longus stabilizing action on the medial column (56). The findings in Part IV suggest that open kinetic chain range of motion of the first ray is a blend of motions of joints comprising the medial column (57). The present study aims to further characterize the contribution of equinus deformity in first ray pathomechanics and focuses on the compensation patterns using a weight bearing cadaver model. We wanted to determine the effect of increased Achilles tension (equinus) on first ray mechanics, particularly how it affects peroneus longus' stabilizing action on the first ray.

Materials and Methods

This research design has been presented previously in more detail (54) and is summarized as follows.

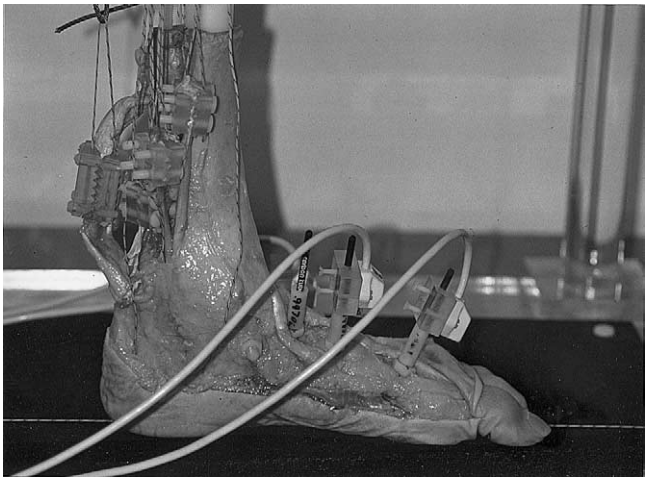

FIGURE 1 Test specimen with cables attached to the tendons of midstance, and Polhemus 3 Space Fastrak sensors attached to osseous segments.

The 7 fresh cadaver lower limb specimens used for this investigation were of mean age 84.1 years at time of death, ranging from 76 to 94 years (3 male, 4 female). Screening was performed by radiography and by visual inspection for abnormal joint space narrowing, significant alignment abnormalities of the medial column and rearfoot, and poor bone stock. Specimens without gross arch height abnormalities were accepted for investigation. The skin, soft tissue and muscle were removed from around the leg and dorsal foot, preserving the posterior leg tendons, ligaments, interosseous membrane, and all plantar soft tissues of the foot. Each specimen was transected 15 to 20 cm proximal to the ankle joint and mounted on a nonmetallic, custom loading frame (designed by BioConcepts Inc., Seattle, WA, and fabricated by Advanced Biomedical, Inc, Oakland, CA). A central rod applied downward load to the tibia and fibula by means of a pneumatic actuator.

Six additional pneumatic actuators applied upward pull on the tendons of midstance. These tendons included peroneus longus, peroneus brevis, Achilles, tibialis posterior, flexor hallucis longus, and flexor digitorum longus. The tendons were anchored to the actuators through non-metallic, serrated tendon clamps and cables (braided Dacron cord of Western Filament, Inc, Grand Junction, CO). Relative forces placed on each tendon were determined using Brand's calculation of physiological cross-sectional area of muscles of midstance (58). Within each trial, the Achilles tendon load was varied at 0, 30, and 60% of predicted maximum load. The remaining five tendons were simultaneously loaded to the predicted maximum load in a constant manner throughout testing (Fig 1).

Sensors were rigidly attached to the first metatarsal, medial cuneiform, navicular, and talus. To monitor the position of the osseous segments of the medial column, a three-dimensional motion tracking system (3 Space Fastrak; Polhemus Inc, McDonnell Douglas Electronics, Colchester, VT), consisting of a magnetic field source and four field sensors, was used. The radio wave tracking system monitored the three-dimensional position of each of the sensors relative to the center of the source (three translations and three rotations). To determine the translations and rotations, a right-handed coordinate system was established that originated at the center of the source box placed superior, posterior, and lateral to the specimen. The positive x axis was directed anteriorly, with rotation about this axis in the frontal plane. The positive y axis was directed medially (for a left foot), with rotation about this axis in the sagittal plane. The positive z axis was directed inferiorly, with rotation about this axis in the transverse plane. The data collected was stored on computer files.

Using a custom loading x-ray apparatus, a position-controlled lateral radiograph of each test specimen was obtained with 222 N of load applied axially. The x-ray beam was precisely aimed at the dorsal aspect of the naviculocuneiform joint for each specimen. The lateral radiograph was used to establish a tarsal index as described by Benink (59). This classified the foot type for each of the specimens tested and defined the arch structure variability of the test group.

Experimental Sequence

Downward load of 400 N was applied to each specimen while the tendons of midstance were loaded. The Achilles tendon load was varied at 0%, 30%, and 60% of predicted maximum load. Three-dimensional data were recorded for the position and orientation of the bone segments as the Achilles tendon load was increased. The sequence was repeated a second time to insure data reproducibility.

Statistical Analysis

The output of the motion tracking system (6 positional coordinates from each sensor) was converted to a global coordinate system on a personal computer using a custom software program and a commercial statistical package. Computer statistical analyses were performed with use of a one-way analysis of variance (ANOVA) with post hoc testing using Scheffe's Multiple Comparisons Test for significant values at $P < .05$ (Statview 4.0; Abacus Systems, Berkeley, CA).

Results

First Metatarsal Motion

First metatarsal rotational orientations of loaded foot specimens with varied Achilles tension were recorded in all

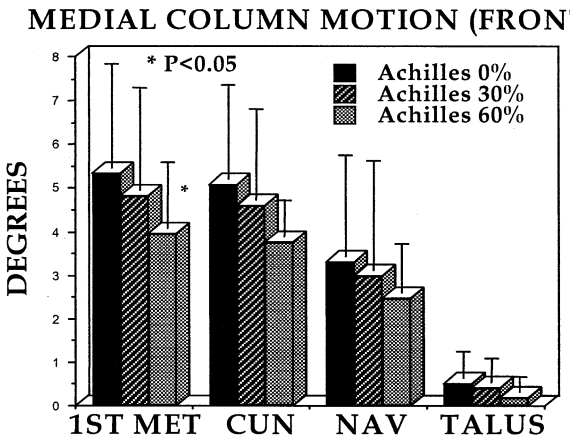

FIGURE 2 Bar graph of medial column motion in the frontal plane with increasing Achilles load. Positive values correlate with eversion direction.

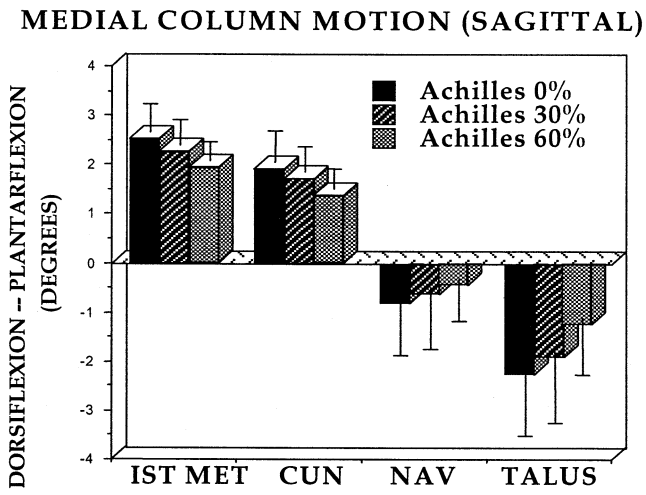

FIGURE 3 Bar graph of medial column motion in the sagittal plane with increasing Achilles load. Positive values correlate with dorsiflexion direction.

three cardinal planes. As Achilles load increased, the position of the first metatarsal became significantly more inverted by 25.8% ($P < .05$).

Frontal Plane. At Achilles load of 0%, a 5.32° ± 2.39° everted position of the first metatarsal occurred. At 30% Achilles load, a 4.81° ± 2.34° everted position of the first metatarsal resulted. At 60% Achilles load, a 3.95° ± 1.52° everted position of the first metatarsal occurred (Fig 2).

Sagittal Plane. At Achilles load of 0%, a 2.53° ± 0.6° plantarflexed position of the first metatarsal occurred. At 30% Achilles load, a 2.29° ± 0.51° plantarflexed position of the first metatarsal resulted. At 60% Achilles load, a 1.97° ± 0.37° plantarflexed position of the first metatarsal occurred (Fig 3).

Transverse Plane. At Achilles load of 0%, a 0.98° ± 1.26° adducted position of the first metatarsal occurred. At 30% Achilles load, a 0.95° ± 1.28° adducted position of the first metatarsal resulted. At 60% Achilles load, a 0.95° ± 0.95° adducted position of the first metatarsal occurred. Linear displacements of the first metatarsal with varied Achilles load were minimal and not statistically significant.

Medial Cuneiform Motion

Medial cuneiform rotational orientations of loaded foot specimens with varied Achilles tension were recorded in all three cardinal planes. As Achilles load increased, a trend was observed such that a 26.8% increase in inversion and 28.9% increase in dorsiflexion of the medial cuneiform occurred.

Frontal Plane. At Achilles load of 0%, a 5.08° ± 2.16° everted position of the medial cuneiform occurred. At 30% Achilles load, a 4.58° ± 2.11° everted position of the medial cuneiform resulted. At 60% Achilles load, a 3.76° ± 0.83° everted position of the medial cuneiform occurred (Fig 2).

Sagittal Plane. At Achilles load of 0%, a 1.94° ± 0.64° plantarflexed position of the medial cuneiform occurred. At 30% Achilles load, a 1.74° ± 0.52° plantarflexed position of the medial cuneiform resulted. At 60% Achilles load, a 1.38° ± 0.41° plantarflexed position of the medial cuneiform occurred (Fig 3).

Transverse Plane. At Achilles load of 0%, a 1.10° ± 0.65° abducted position of the medial cuneiform occurred. At 30% Achilles load, a 1.20° ± 0.82° abducted position of the medial cuneiform resulted. At 60% Achilles load, a 1.13° ± 0.44° abducted position of the medial cuneiform occurred. Linear displacements of the medial cuneiform with varied Achilles load were minimal and not statistically significant.

Navicular Motion

Navicular rotational orientations of loaded foot specimens with varied Achilles tension were recorded in all three cardinal planes. As Achilles load increased, a trend was observed such that a 24.8% increase in inversion of the navicular occurred. Only a slight trend of plantarflexion and adduction in sagittal and transverse planes, respectively, was detected.

Frontal Plane. At Achilles load of 0%, a 3.30° ± 2.31° everted position of the navicular occurred. At 30% Achilles load, a 2.99° ± 2.49° everted position of the navicular resulted. At 60% Achilles load, a 2.48° ± 1.11° everted position of the navicular occurred (Fig 2).

Sagittal Plane. At Achilles load of 0%, a 0.81° ± 1.18° dorsiflexed position of the navicular occurred. At 30%

Achilles load, a 0.60° ± 1.25° dorsiflexed position of the navicular resulted. At 60% Achilles load, a 0.45° ± 0.86° dorsiflexed position of the navicular occurred (Fig 3).

Transverse Plane. At Achilles load of 0%, a 1.97° ± 0.56° abducted position of the navicular occurred. At 30% Achilles load, a 1.94° ± 0.48° abducted of the navicular position resulted. At 60% Achilles load, a 1.70° ± 0.42° abducted position of the navicular occurred.Linear displacements of the navicular with varied Achilles load were minimal and not statistically significant.

Talar Motion

Talar rotational orientations of loaded foot specimens with varied Achilles tension were recorded in all three cardinal planes. As Achilles load increased, a definite trend was detected such that a 43.7% increase in plantarflexion and a 14.0% increase in adduction occurred. However, this difference was not statistically significant. Minimal change of talar position occurred in the frontal plane.

Frontal Plane. At Achilles load of 0%, a 0.51° ± 0.62° everted position of the talus occurred. At 30% Achilles load, a 0.41° ± 0.55° everted position of the talus resulted. At 60% Achilles load, a 0.20° ± 0.34° everted position of the talus occurred (Fig 2).

Sagittal Plane. At Achilles load of 0%, a 2.24° ± 1.38° dorsiflexed position of the talus occurred. At 30% Achilles load, a 1.91° ± 1.45° dorsiflexed position of the talus resulted. At 60% Achilles load, a 1.26° ± 1.14° dorsiflexed position of the talus occurred (Fig 3).

Transverse Plane. At Achilles load of 0%, a 2.85° ± 1.37° abducted position of the talus occurred. At 30% Achilles load, a 2.59° ± 1.06° abducted position of the talus resulted. At 60% Achilles load, a 2.45° ± 0.77° abducted position of the talus occurred. Linear displacements of the talus with varied Achilles load were minimal and not statistically significant.

Arch Height Calculations

Benink's tarsal index formula (60) was used to calculate the arch height of each specimen. The tarsal index for the seven specimens ranged from 2.1 to 10.7, with a mean of 5.8 ± 2.9. This is an above average arch height. There was no correlation between arch height and the effect of Achilles action. However, the sample size was small and the effect of arch height on Achilles function could not be determined.

Discussion

Using electrical stimulation techniques, Duchenne analyzed the function of the triceps surae (24). His most profound discovery involved the forcible plantarflexion of the lateral column while the medial column yielded to the slightest resistance. This finding was further reinforced by his determination that pure foot plantarflexion required combined stimulation of peroneus longus with triceps surae. He determined that there was an antagonistic relationship between triceps surae and peroneus longus which is supported in the present investigation. In closed kinetic chain, Achilles preload from equinus deformity will magnify forefoot load to the lateral column and indirectly resist the action of peroneus longus via ground reaction.

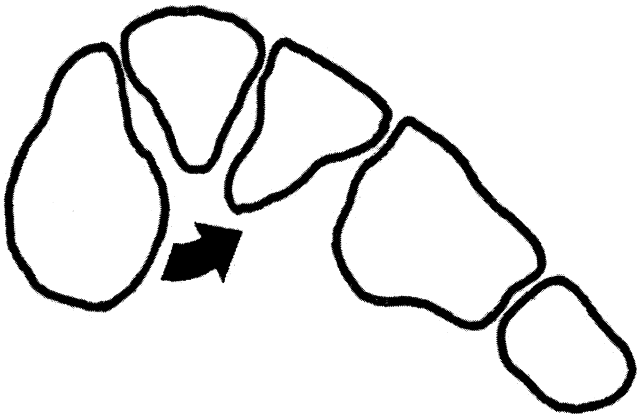

FIGURE 4 Cross section of osseous segments of midfoot illustrating eversion influence of peroneus longus on the medial column. This action is dampened with increased tension on the Achilles tendon.

The closed kinetic chain effects of peroneus longus activity on the medial column of the foot were investigated previously (54). Significant frontal plane rotation of the medial column in the direction of eversion occurred when peroneus longus load was increased ($P = .0001$). Increasing peroneus longus loads produced smaller but significant angular changes in the sagittal and transverse planes of the medial column. The patterns of motion found suggest that peroneus longus creates an eversion "locking" effect on the first ray of the foot, stabilizing the medial column.

In the present study, the most demonstrable difference with increased Achilles load was observed in the frontal plane. By dampening frontal plane function of peroneus longus, equinus apparently affects the locking mechanism of the medial column (Fig 4). Many clinicians believe that equinus deformity leads to first ray hypermobility. This is often thought to be purely a function of the gradual stretching of the plantar ligaments due to downward pressure on the arch as described by Morton (47). However, this investigation suggests that equinus reduces peroneus longus locking influence of the first ray which may also lead to hypermobility.

Equinus deformity has also been implicated in the pathogenesis of acquired flatfoot deformity. Schuster described

the effect of a shortened gastrocnemius as a bending of the rearfoot on the forefoot, which he termed "secondary flexion" (20). Similarly, Morton described a crushing force through the talus that affects the structures forming the longitudinal arch. He felt this resulted in an altered position of the navicular with the first metatarsal being forced directly into heavier contact with the ground (28, 47). Both Schuster's and Morton's descriptions were confirmed by the three dimensional kinematic results of this study. As Achilles tension increased, a measurable arch flattening effect with plantarflexion of the talus and navicular and dorsiflexion of the first metatarsal and cuneiform was seen (Fig 3). The magnitude of deformity in the current investigation agrees with data from Thordarson et al. However, in their study, the exact level of "arch flattening" was not determined (41). This investigation shows a strong trend toward sagittal plane compensation occurring at the level of the naviculocuneiform joint.

This experimental design has several inherent limitations. The relative tendon loads applied to each specimen can only be estimated. However, in this study, tensions were based on available physiologic muscle data (58). The pathologic loads through the Achilles tendon in equinus deformity as it effects the foot in midstance is unknown. Furthermore, the equinus effects induce a gradual loss of structural integrity that can not be easily replicated in a cadaver model. Despite these limitations, this investigation provides important insights into equinus after-effects, most notably subtle compensatory mechanisms of the intact medial column. Such interactions can not be accurately measured in other experimental designs.

In clinical practice, the early destructive influence of equinus is often not appreciated. Instead, we are usually faced with the end result of equinus effects—be it a bunion condition, a unilateral flatfoot, or a forefoot diabetic ulcer. This investigation, dealing with specimens without deformity, gives us insight into early patterns of compensation for equinus. With dampening of peroneus longus function under early equinus influence, it is understandable that first ray hypermobility and hallux valgus deformity are the end points of the influence. Furthermore, the arch flattening effect seen kinematically with increased tension on the Achilles illustrates why the midfoot is susceptible to equinus forces. Most commonly, the clinical end stage manifests as loss of arch integrity with flatfoot conditions as well as Lisfranc arthrosis (5) and Charcot arthropathy (5, 9). On clinical examination of diabetics with neuropathy, it is not uncommon to observe a tight Achilles tendon. Grant and associates investigated the fine structural changes in the Achilles tendon of patients with long-term diabetes mellitus and found morphologic abnormalities that appear to be the result of nonenzymatic glycosylation (9). In a study of 221 Charcot fractures, Schon et al (60) reported over one-half of the cases involving midfoot collapse. The destructive influence of a progressive equinus deformity can lead to rapid arch collapse and threatens limb function and viability. In another investigation on diabetic ulcers, Armstrong et al (12) concluded that percutaneous Achilles tendon lengthening reduced peak forefoot pressures in a series of patients at high risk for ulcer. Preemptive Achilles tendon lengthening in these high-risk patients could reduce incidence of catastrophic collapse. Further clinical research in this area is needed.

Our findings support the concept that treatment of equinus can slow the development of hallux abductovalgus by reducing first ray hypermobility and allowing peroneus longus to function more effectively. Failure of various arch stabilizing procedures and bunion corrections can often be attributed to an untreated equinus deformity. Likewise, failure to address an equinus deformity may explain persistent arch symptoms in patients after plantar fascial release for plantar fasciitis. The authors strongly recommend careful clinical assessment and appropriate treatment of equinus in patients with biomechanical deformities affecting the first ray and midfoot.

Conclusion

With increasing Achilles load, the influence of peroneus longus on the medial column is diminished. Equinus effects on an intact longitudinal arch seem to affect the distal components of the medial column, primarily in the frontal plane. A measurable arch flattening effect with plantarflexion of the talus and navicular and dorsiflexion of the first metatarsal and cuneiform occurs with increased Achilles pull.

References

1. Harris RI, Beath T. Hypermobile flat-foot with short tendo achillis. J Bone Joint Surg 30A:116, 1948.
2. Barry LD, Barry AN, Chen Y. A retrospective study of standing gastrocnemius-soleus stretching versus night splinting in the treatment of plantar fasciitis. J Foot Ankle Surg 41:221–227, 2002.
3. DiGiovanni CW, Kuo R, Tejwani N, Price R, Hansen T, Cziernecki J, Sangeorzan B. Isolated gastrocnemius tightness. J Bone Joint Surg Am 84A:962–970, 2002.
4. Hill RS. Ankle equinus. Prevalence and linkage to common foot pathology. J Am Podiatr Med Assoc 85:295–300, 1995.
5. Hansen ST Jr. *Functional Reconstruction of the Foot and Ankle*, Lippincott Williams & Wilkins, Philadelphia, 2000.
6. Subotnick SI. Equinus deformity as it affects the forefoot. J Am Podiatry Assoc 61:423–427, 1971.
7. Banks AS, McGlamry ED. Charcot foot. J Am Podiatr Med Assoc 79:213–235, 1989.
8. Downey MS. Ankle Equinus. In *McGlamry's Comprehensive Textbook of Foot and Ankle Surgery,* pp 715–760, edited by AS Banks, MS Downey, DE Martin, SJ Miller, Lippincott Williams & Wilkins, Philadelphia, 2001.
9. Grant WP, Sullivan R, Sonenshine DE, Adam M, Slusser JH, Carson KA, Vinik AI. Electron microscopic investigation of the effects of

diabetes mellitus on the Achilles tendon. J Foot Ankle Surg 36:272–278, discussion 330, 1997.
10. Hansen ST Jr. Hallux valgus surgery. Morton and Lapidus were right. Clin Podiatr Med Surg 13:347–354, 1996.
11. Sgarlato TE, Morgan J, Shane HS, Frenkenberg A. Tendo achillis lengthening and its effect on foot disorders. J Am Podiatry Assoc 65:849–871, 1975.
12. Armstrong DG, Stacpoole-Shea S, Nguyen H, Harkless LB. Lengthening of the Achilles tendon in diabetic patients who are at high risk for ulceration of the foot. J Bone Joint Surg Am 81A:535–538, 1999.
13. Lin SS, Lee TH, Wapner KL. Plantar forefoot ulceration with equinus deformity of the ankle in diabetic patients: the effect of tendo-Achilles lengthening and total contact casting. Orthopedics 19:465–475, 1996.
14. Lavery LA, Armstrong DG, Boulton AJ. Ankle equinus deformity and its relationship to high plantar pressure in a large population with diabetes mellitus. J Am Podiatr Med Assoc 92:479–482, 2002.
15. Green DR, Ruch JA, McGlamry ED. Correction of equinus-related forefoot deformities: a case report. J Am Podiatry Assoc 66:768–780, 1976.
16. Basmajian JV. *Muscles Alive*, ed 4, Williams and Wilkins, Baltimore, 1979.
17. Perry J. *Gait Analysis. Normal and pathological function*, McGraw-Hill, New York, 1992.
18. Crowninshield RD, Brand RA. A physiologically based criterion of muscle force prediction in locomotion. J Biomech 14:793–801, 1981.
19. Root ML, Orien WP, Weed JH. *Clinical Biomechanics. Volume II: Normal and abnormal function of the foot*, Clinical Biomechanics Corporation, Los Angeles, 1977.
20. Schuster OF. *Foot Orthopaedics*, Marbridge Printing, New York, 1927.
21. Baggett BD, Young G. Ankle joint dorsiflexion. Establishment of a normal range. J Am Podiatr Med Assoc 83:251–254, 1993.
22. Bohannon RW, Tiberio D, Zito M. Selected measures of ankle dorsiflexion range of motion: differences and intercorrelations. Foot Ankle 10:99–103, 1989.
23. D'Amico JC. Equinus: identification and clinical significance. Arch Podiatr Med Foot Surg 4:10, 1977.
24. Duchenne GB. *Physiologie des Mouvements*, Lippincott, Philadelphia, 1867.
25. Ekstrand J, Gillquist J. The frequency of muscle tightness and injuries in soccer players. Am J Sports Med 10:75–78, 1982.
26. Gottlieb A. Flatfoot and its relation to the triceps surae muscle. Am J Phys Ther 8:321–323, 1932.
27. Hillstrom HJ, Perlberg G, Siegler S, Sanner WH, Hice GA, Downey M, Stienstra J, Acello A, Neary MT, Kugler F. Objective identification of ankle equinus deformity and resulting contracture. J Am Podiatr Med Assoc 81:519–524, 1991.
28. Morton DJ. Mechanism of the normal foot and of flat foot. J Bone Joint Surg 6:368–406, 1924.
29. Oberg B, Ekstrand J, Moller M, Gillquist J. Muscle strength and flexibility in different positions of soccer players. Int J Sports Med 5:213–216, 1984.
30. Root ML, Orien WP, Weed JH. *Clinical Biomechanics. Volume I: Examination of foot*, Clinical Biomechanics, Los Angeles, 1971.
31. Stauffer RN, Chao EY, Brewster RC. Force and motion analysis of the normal, diseased, and prosthetic ankle joint. Clin Orthop 127:189–196, 1977.
32. Walsh WM, Blackburn T. Prevention of ankle sprains. Am J Sports Med 5:243–245, 1977.
33. Wiktorsson-Moller M, Oberg B, Ekstrand J, Gillquist J. Effects of warming up, massage, and stretching on range of motion and muscle strength in the lower extremity. Am J Sports Med 11:249–252, 1983.
34. Lapidus PW. The operative correction of metatarsus varus primus in hallux valgus. Surg Gynecol Obstet 58:183–191, 1934.
35. Lapidus PW. A quarter of a century of experience with the operative correction of the metatarsus varus in hallux valgus. Bull. Hosp Joint Dis Orthop Inst 17:404–421, 1956.
36. Lapidus PW. The author's bunion operation from 1931 to 1959. Clin Orthop 16:119–135, 1960.
37. Shaffer NM. Flatfoot: its causes and treatment. New York Med J 65:717–721, 1897.
38. Sgarlato TE. *A Compendium of Podiatric Biomechanic,* California College of Podiatric Medicine, San Francisco, 1971.
39. Flinchum D. Pathological anatomy in talipes equinovarus. J Bone Joint Surg 35A:111–114, 1953.
40. Melillo TV. Gastrocnemius equinus: its diagnosis and treatment. Arch Podiatr Med Foot Surg 2:159–205, 1975.
41. Thordarson DB, Schmotzer H, Chon J, Peters J. Dynamic support of the human longitudinal arch. A biomechanical evaluation. Clin Orthop 316:165–172, 1995.
42. Sutherland DH. An electromyographic study of the plantar flexors of the ankle in normal walking on the level. J Bone Joint Surg 48A:66–71, 1966.
43. Murray MP, Guten GN, Baldwin JM, Gardner GM. A comparison of plantar flexion torque with and without the triceps surae. Acta Orthop Scand 47:122–124, 1976.
44. Simon SR, Mann RA, Hagy JL, Larsen LJ. Role of the posterior calf muscles in normal gait. J Bone Joint Surg 60A:465–472, 1978.
45. Morton DJ. Hypermobility of the first metatarsal bone. J Bone Joint Surg 10:187–196, 1928.
46. Morton DJ. Structural factors in static disorders of the foot. Am J Surg 9:315–328, 1930.
47. Morton DJ. *The Human Foot: Its Evolution, Physiology and Functional Disorders*, Columbia University Press, Morningside Heights, 1935.
48. Hicks JH. The mechanics of the foot. Anatomy 87:345–357, 1953.
49. Kelikian H. *Hallux Valgus, Allied Deformities of the Forefoot and Metatarsalgia*, Saunders, Philadelphia, 1965.
50. Kelso SF, Richie DH Jr, Cohen IR, Weed JH, Root M. Direction and range of motion of the first ray. J Am Podiatr Assoc 72:600–605, 1982.
51. Kitaoka HB, Lundberg A, Luo ZP, An KN. Kinematics of the normal arch of the foot and ankle under physiologic loading. Foot Ankle Int 16:492–499, 1995.
52. Klaue K, Hansen ST, Masquelet AC. Clinical, quantitative assessment of first tarsometatarsal mobility in the sagittal plane and its relation to hallux valgus deformity. Foot Ankle Int 15:9–13, 1994.
53. Wanivenhaus A, Pretterklieber M. First tarsometatarsal joint: anatomical biomechanical study. Foot Ankle 9:153–157, 1989.
54. Johnson CH, Christensen JC. Biomechanics of the first ray. Part I. The effects of peroneus longus function: a three-dimensional kinematic study on a cadaver model. J Foot Ankle Surg 38:313–321, 1999.
55. Rush S, Christensen JC, Johnson CH. Biomechanics of the first ray. Part II: Metatarsus primus varus as a cause of hypermobility. A three-dimensional kinematic analysis in a cadaver model. J Foot Ankle Surg 39:68–77, 2000.
56. Bierman RA, Christensen JC, Johnson CH. Biomechanics of the first ray. Part III. Consequences of Lapidus arthrodesis on peroneus longus function: a three-dimensional kinematic analysis in a cadaver model. J Foot Ankle Surg 40:125–131, 2001.
57. Roling BA, Christensen JC, Johnson CH. Biomechanics of the first ray. Part IV: the effect of selected medial column arthrodeses. A three-dimensional kinematic analysis in a cadaver model. J Foot Ankle Surg 41:278–285, 2002.
58. Brand RA, Pedersen DR, Friederich JA. The sensitivity of muscle force predictions to changes in physiologic cross-sectional area. J Biomech 19:589–596, 1986.
59. Benink RJ. The constraint-mechanism of the human tarsus. A roentgenological experimental study. Acta Orthop Scand 215(suppl):1–135, 1985.
60. Schon LC, Easley ME, Weinfeld SB. Charcot neuroarthropathy of the foot and ankle. Clin Orthop 349:116–131, 1998.